High-pressure MOCVD growth for thick InGaN films toward the photovoltaic applications

Liwen Sang[1,2,*], Masatomo Sumiya[3], Meiyong Liao[3], Xuelin Yang[4], and Bo Shen[4]

[1] International Center for Materials Nanoarchitectonics (MANA), National Institute for Materials Science (NIMS), 1-1 Namiki, Tsukuba, Ibaraki 305-0044, Japan

[2] JST-PRESTO, The Japan Science and Technology Agency, Tokyo 102-0076, Japan.

[3] Research Center for Functional Materials, National Institute for Materials Science, 1-1 Namiki, Tsukuba, Ibaraki 305-0044, Japan

[4] State Key Laboratory of Artificial Microstructure and Mesoscopic Physics, School of Physics, Peking University, Beijing, China

E-mail: SANG.Liwen@nims.go.jp

Abstract

The highly efficient photovoltaic cells require the In-rich InGaN film with a thickness more than 300 nm to obtain the enough photo·electricity energy conversion. However, the InGaN thick films suffer from poor crystalline quality and phase separations by using the conventional metal organic chemical vapor deposition (MOCVD). We report on the growth of 0.3-1 μm-thick InGaN films by using a specially designed vertical-type high-pressure MOCVD at the pressure up to 2.5 atms. The In incorporation is found to be greatly enhanced at the elevated pressures although the growth temperatures are the same. The phase separations are inhibited when the growth pressure is higher than atmospheric pressure, leading to the improved crystalline quality and better surface morphologies especially for the In-rich InGaN. The $In_{0.4}Ga_{0.6}N$ with the thickness of 300 nm is further utilized as the active region for solar cells, and the wide-range photoresponse from ultraviolet to more than 700 nm is achieved.

1. Introduction

The ternary alloy indium-gallium-nitride (InGaN) is the main building block for the optoelectronic devices, such as light emitting diodes (LEDs), laser diodes (LDs), solar cells, photodiodes, etc. In particular, InGaN has the tunable direct band gaps from 0.7 to 3.4 eV by changing In composition, covering almost all the solar spectrums, which has been attracting great interests for the high efficiency photovoltaic applications [1,2]. Moreover, their high absorption coefficients (~10^5/cm), high thermal/chemical stability, and superior radiation robustness allow the operations in the extreme conditions such as in the space or terrestrial application [3-7]. For the InGaN solar cells to obtain efficient absorption from the incident light, the thickness of the active region should be higher than 300 nm [5]. Unfortunately, it is difficult to obtain high-quality thick InGaN films by the conventional low-pressure metal organic chemical vapor deposition (MOCVD) when the In mole fraction is higher than 20% due to the alloy disorder and phase separation [8-10]. Up to now, most of the InN and In-rich InGaN films are grown by molecular beam epitaxy (MBE), but they are still far from the device applications compared to the MOCVD growth. In the conventional and commercial MOCVDs, the systems are all designed for the pressure lower than atmospheric pressure (1 atm), and to improve the In mole fractions, the growth temperature was particularly low. However, at low growth temperatures, the decomposition of ammonia is insufficient and the surface morphology of InGaN is degraded due to the low migration of atoms [11]. Therefore, the thickness was restricted to be lower than 100 nm especially for the In-rich InGaN, which is far from the requirement for the solar cells [8-10]. An alternative method by using InGaN/GaN multiple quantum wells (MQWs) to replace the thick InGaN films can improve the quality of the active region, while its external quantum efficiency (EQE) is far from the expected

value due to the insufficient absorption of the sun light [12,13]. More importantly, the optical absorption of the current solar cells either with InGaN films or MQWs is concentrated on the short wavelength lower than 450 nm due to the low In composition [12-15]. To achieve the practical photovoltaic efficiencies greater than 50% as indicated by the detailed-balance model, the absorption energies should be greater than 2.4 eV, which requires the InGaN to have an In more fraction more than 40% [6,7]. Therefore, to ultimate improve the conversion efficiency of the InGaN-based solar cells, the high-quality $In_xGa_{1-x}N$ films with the thickness higher than 300 nm and In composition more than 40% are required.

Base on the equilibrium pressure-temperature relationship for the III-V nitride semiconductors, InN decomposes at a much lower temperature than GaN, and increasing the nitrogen vapor pressure can reduce the decomposition of InN. Therefore, the high growth pressure enables a high growth temperature for the InGaN, at which the surface morphology and crystalline quality are expected to be improved. Studies on the growth of InGaN by using MOCVD with the pressure up to 200 kPa (~2 atms) was reported, but the crystalline qualities and surface morphologies were not shown [16]. In addition, there is no report on the device applications using the InGaN films grown by using the high-pressure MOCVD.

In this work, we report on the thick InGaN films (0.3-1 μm) grown at the pressure up to 2.5 atms using a specially designed vertical-type high-pressure MOCVD (HPMOCVD). It was found that the In incorporation was greatly enhanced with the pressure increasing although the growth temperature was the same. The phase separation was also restricted when the pressure was raised more than 1 atm especially when the In composition is higher than 30%. The solar cells with the light absorption as long as 700

nm was demonstrated using the thick InGaN grown at 1.5 atms as the active region, which will be promising for the high-efficiency photovoltaic applications.

2. Material and methods

The InGaN films with the thickness of 0.3-1 μm were grown on the epi-ready *c*-plane GaN/sapphire template by using a specially designed vertical-type HPMOCVD which can be operated up to 3 atms. The close coupled showerhead reactors were designed to improve the homogeneity of InGaN. The trimethylgallium (TMGa), trimethylindium (TMIn), and ammonia were utilized as the Ga, In and N sources, respectively. The growth pressures were varied from 0.5 to 2.5 atms under the growth temperature from 830 to 680 °C to achieve different In mole fractions. The growth temperature was measured using a thermocouple positioned at the center of the heater. Nitrogen was used as the carrier gas. The In mole fraction was determined by X-ray diffraction (Panalytical Xpert PRO XRD system), and surface morphology was evaluated by atomic force microscopy (AFM). The Hall effect measurement with a Van der Pauw method was used to determine the electron concentration and mobility of the InGaN films. For the solar cells, a 300 nm-thick $In_xGa_{1-x}N$ (x~0.4) grown at the pressure of 1.5 atms on the *n*-$In_{0.15}Ga_{0.85}N$ were used as the active region, followed by the p-$In_{0.15}Ga_{0.85}N$/p-GaN region at the pressure of 1 atm. The solar cell devices were fabricated using a standard semiconductor processing technique. Current-voltage (*I-V*) characteristics were measured with a Keitheley 2635B source meter. The solar cell performance was evaluated under air mass (AM) 1.5 (100 mW/cm^2) illumination condition using a xenon-arc light source (Wacom Electric HX-504/Q). The EQE of the samples was evaluated from a standard lock-in detection technique from 800 nm to 300 nm with a 500 W xenon lamp.

3. Results

Figure 1 (a) shows the XRD 2θ-ω scan curve in the (002) direction for the InGaN

grown at the pressure of 1 atm and the temperature of 880 °C using the high-pressure MOCVD system. The thickness of the film was measured to be 900 nm by scanning electron microscopy (SEM), as indicated in the inset of Fig. 1 (a). The major sharp peak in Fig. 1 (a) corresponds to the diffraction from the GaN template, and the secondary peak on the left indicate the strong diffraction from the InGaN film. Except for the main diffraction peaks, the clear interference fringes around InGaN peak are observed, which indicates an ultra-flat interface between GaN and InGaN. The In mole fraction is estimated to be 5%. The surface of the obtained $In_{0.05}Ga_{0.95}N$ exhibits clear atomic steps, as shown in the AFM image of Fig. 1 (b). The root-mean square roughness (rms) is ~0.2 nm, and no hexagonal pits are observed on the surface even for the thickness of 900 nm. Figures 1 (c) and (d) are the rocking curves of the InGaN peak around (002) and (101)-plane, respectively. The full width at half maximum (FWHM) value is 104 arcsec for (002)-plane and 374 arcsec for (101)-plane, showing a good crystalline quality. From Hall effect measurement, the electron mobility of the obtained $In_{0.05}Ga_{0.95}N$ film is 148 cm^2/Vs with a carrier concentration of ~$10^{17}/cm^3$, indicating a good electrical property.

The growth temperatures were then reduced to improve the In incorporation in the InGaN grown by the HPMOCVD. Figure 2 (a) shows the dependence of the In mole fraction in the InGaN film grown at the pressure from 0.5 to 2.5 atms under the same temperature of 830 °C. As can be seen, the In mole fractions display a nearly linear increase with the growth pressures. At 0.5 atm, a typical growth pressure used in the conventional MOCVD, the In mole fraction of the InGaN film is ~ 6%. This value is drastically increased to ~39% when the pressure is increased to 2.5 atms although the growth temperatures are the same. While the growth rates are found to be greatly reduced at high pressures, as shown in Fig. 2 (b). When the pressure is increased, the growth

process is mainly affected by nucleation of gas phases. The formation of nanoparticles from the nucleation depends on the residence time, which is longer at high pressures, thus enhancing the parasitic reaction. The parasitic reaction reduces the particle density on the surface, then decreases the surface reaction and lowers the growth rates. Such a trend is consistent with other reports in the commercial MOCVD chamber [17,18]. The electron concentrations and mobilities of the InGaN films with the In mole fraction of ~30% grown at different pressures are compared in Figs. 2 (c) and (d). The growth temperatures were varied to keep the similar In incorporation. As can be seen, all the InGaN films show the electron mobility higher than 120 cm^2/Vs. A highest mobility of 193 cm^2/Vs is achieved for the $In_{0.32}Ga_{0.68}N$ film with a thickness of 500 nm at the growth pressure of 1.5 atms. The electron concentration is increased with the pressure increasing, which is due to the impurity incorporation from the low migration of reaction atoms at high pressures.

The crystalline qualities of the InGaN films are further evaluated by the XRD rocking curves. Figure 3 shows the full width at half maximum (FWHM) values of the XRD rocking curves for the (002) and (101)-plane as a function of the In mole fractions at different growth pressures. The In-rich InGaN are obtained at the pressure higher than atmospheric pressure while the In mole fractions are relatively lower at the pressure of 0.5 atm. The FWHMs are increased with the In composition increasing in InGaN films. When the In composition is lower than 20%, the crystalline quality shows little dependence on the growth pressures. Nevertheless, when the In mole fraction is higher than 20%, the InGaN films grown at 2 atms have the smaller FWHM values than those grown at 1 atm for both the (002) and (101) planes. This result indicates the advantage by using the high-pressure growth for the In-rich InGaN films.

Except for the XRD properties, the phase separations in the In-rich InGaN films are found to be drastically inhibited at high-pressure growth conditions. During the MBE and low-pressure MOCVD growth for InGaN, the phase separations have been widely reported as a result of the higher vapor pressure of nitrogen [8,10,19]. The XRD curves of the (002)-plane for the InGaN films grown at different temperatures are illustrated in Figs. 4 (a1) and (b1) at the growth pressure of 1 and 2 atms, respectively. The In mole fractions are estimated to be 30-50%. As can be seen, when the growth pressure is 1 atm at the temperature of 720 °C, two peaks corresponding to the diffraction of InGaN are observed at 34.0° and 33.5°, showing the phase separation of InGaN film during the growth even the temperature was not varied. The peak at 32.9° is generated by the In droplets on the surface [20]. It is also noted that the surface of the InGaN film was degraded with large grain boundaries, as shown in the AFM image of Fig. 4 (a2). The rms is around 13.9 nm. When the temperature is further reduced, the phase separation becomes serious and the InGaN diffraction peaks become wider. The surface morphology is even more deteriorated, and the rms is increased to be ~ 28.2 nm at the growth temperature of 720 °C. On the other hand, no phase separation from XRD is detected for the InGaN films grown at the pressure of 2 atms (Fig. 4 (b1)). The In mole fraction of 36% is achieved for InGaN film at the temperature over 820°C, along with a good surface morphology with the rms of ~ 0.57 nm, as displayed in Fig. 4 (b2). When the temperature is reduced to 780 °C and In mole fraction is 41%, atomic steps are still detectable on the surface by AFM while the hexagonal pits appear (Fig. 4 (b3)). This is because of the generation of threading dislocations with In mole fraction increasing. When the In composition is further increased to 46% at the temperature of 760 °C, the intensity from XRD diffraction is reduced and the surface morphology starts to be degraded and grain

boundary appears (Fig. 4 (b3)).

The performances of solar cells were characterized with regard to the optical and electrical analysis. The photocurrent spectrum showing the absorption behavior of the solar cell exhibits the wide-range response from ultraviolet to the long-wavelength of >700 nm. The EQE (number of electrons produced as photocurrent per incident photon for the different wavelength [21]) as a function of excitation wavelength is shown in Fig. 5 (a). It is revealed that the device delivers a peak quantum efficiency of 37% at 576 nm. The EQE is enhanced compared to the solar cell with a thin $In_{0.4}Ga_{0.6}N$ layer using the conventional MOCVD in our group [22]. The short-circuit current density (J_{sc}) is 1.62 mA/cm^2 with an open-circuit voltage (V_{oc}) of 1.3V, when the devices are measured under AM 1.5 solar simulator illumination (Fig. 5 (b)). The shunt resistance of the device is 620 Ωcm^2, which is relatively low. This is probably because of the higher leakage current as a result of the structural defects in the In-rich InGaN or the damage from device fabrication. In addition, the serial resistance is estimated to be 429 Ωcm^2. The influence on the serial resistance is usually considered from the high resistivity of the contacts or the low carrier concentration in the *p*-type region. The fill factor (FF) is determined to be 40 %, with a conversion efficiency (η) of 0.82%. We also found that, further optimization on the *p*-type region will improve the performance of the InGaN solar cells, for example, an In composition gradient *p*-InGaN to improve the hole mobility [22].

4. Summary

The InGaN films with the thickness of 0.3-1 μm and In mole fractions from 0 to 50% are successfully obtained using a specially designed vertical-type HPMOCVD. With the growth pressure elevated, the In incorporation was found to be drastically enhanced compared to those at the low-pressure conditions when the growth temperatures are the

same. It is revealed that, the phase separation issue, which typically occurs for In-rich InGaN during the growth using MBEs or conventional low-pressure MOCVDs, can be successfully inhibited when the growth pressure is raised to 2 atms. The FWHMs of InGaN films for both (002) and (101)-planes are reduced at the high growth pressures, especially when the In mole fraction is more than 20%. The 300 nm-thick InGaN film grown using the high-pressure MOCVD is further utilized as the active region of solar cells, and a wide-range photoresponse from ultraviolet to > 700nm is achieved, covering the strongest absorption of the sun light. This work provides a new route for the growth of the high-quality In-rich InGaN thick films at the high-pressure conditions through modifying the MOCVD system, and will be helpful for the development of the high-efficiency photovoltaics.

ACKNOWLEDGMENTS

This work was supported by the JST-PRESTO Grant No. JPMJPR19I7, and World Premier International Research Center (WPI) initiative on Materials Nanoarchitectonics (MANA), Ministry of Education, Culture, Sports, Science & Technology (MEXT) in Japan. The authors thank Cho Yujin for her kind support on the CL measurements.

Reference:

[1] T. Kawashima, H. Yoshikawa, S. Adachi, S. Fuke, and K. Ohtsuka, “Optical properties of hexagonal GaN,” J. Appl. Phys., vol. 82, no. 7, pp. 3528–3535, Oct. 1997.

[2] J. Wu, W. Walukiewicz, W. Shan, K. M. Yu, J. W. Ager, S. X. Li, E.E. Haller, H. Lu, and W. J. Schaff, “Temperature dependence of the fundamental band gap of InN,” J. Appl. Phys., vol. 94, no. 7, pp. 4457–4460, Oct. 2003.

[3] A. David, M. Grundmann, “Influence of polarization fields on carrier lifetime and recombination rates in InGaN-based light-emitting diodes,” Appl. Phys. Lett., vol. 97, pp. 033501-1–033501-3, May 2010.

[4] J. Wu, W. Walukiewicz, K. M. Yu, W. Shan, and J. W. Ager III, “Superior radiation resistance of In1−x GaxN alloys: Full solar-spectrum photovoltaic material system,” J. Appl. Phys., vol. 94, no. 10, pp. 6477–6482, Jun. 2013.

[5] Liwen Sang, Meiyong Liao, Yasuo Koide, Masatomo Sumiya, InGaN-based thin film solar cells: Epitaxy, structural design, and photovoltaic properties. Journal of Applied Physics. 117, 105706 (2015)

[6] U. K. Kumawat, K. Kumar, P. Bhardwaj, and A. Dhawan, Indium-rich InGaN/GaN solar cells with improved performance due to plasmonic and dielectric nanograting, Energy Science & Engineering, 7, 2469-2482, 2019

[7] C. Hongsberg, O. Ferguson, D. Nicol, A. Payne, “InGaN-A New Solar Cell Material”, Proceedings of the 19th European Photovoltaic Science and Engineering Conference, Paris, France, June 7-11, 2004, p.15-20.

[8] B. N. Pantha, J. Li, J. Y. Lin, and H. X. Jiang, Single phase InxGa1-xN ($0.25 \leq x \leq 0.63$) alloys synthesized by metal organic chemical vapor deposition, Appl. Phys. Lett. 93, 182107 (2008)

[9] S. Y. Karpov, MRS Internet J. Nitride Semicond. Res. 3 16 (1998)

[10] M. Shimizu, Y. Kawaguchi, K. Hiramatsu, and N. Sawaki, Metalorganic Vapor Phase Epitaxy of Thick InGaN on sapphire substrate, Jpn. J. Appl. Phys. 36, 3381 (1997)

[11] A. Koukitsu, N. Takahashi, T. Taki, and H. Seki, Thermodymanic analysis of the MOVPE growth of $In_xGa_{1-x}N$, J. Crys. Growth, 170, 306-311 (1997)

[12] R. Dahal, B. Oantha, J. Li, J. Y. Lin, and H. X. Jiang, InGaN/GaN multiple quantum

well solar cells with long operating wavelengths, Appl. Phys. Lett. 94, 063505 (2009)

[13] Liwen Sang, Meiyong Liao, Naoki Ikeda, Yasuo Koide, Masatomo Sumiya. Enhanced performance of InGaN solar cell by using a super-thin AlN interlayer. Applied Physics Letters. 99, 161109 (2011)

[14] M. Sumiya, T. Honda, L. Sang, Y. Nakano, K. Watanabe, and F. Hasegawa, Phys. Status Solidi A, 212, 1033-1038 (2015)

[15] A. G. Bhuiyan, K. Sugita, A. Hashimoto, and A. Yamamoto, InGaN solar cells: Present state of the Art and Important challenges, IEEE Journal of photovoltaics, 2, 276 (2012)

[16] D. Iida, et al. Appl. Phys. Express 3, 075601 (2010)

[17] S. Hu, S. Liu, Z. Zhang, H. Yan, Z. Gan, H. Fang, A novel MOCVD reactor for growth of high-quality GaN-related LED layers, J. Crys. Growth, 415, 72-77 (2015)

[18] M. Dauelsberg, C. Martin, H. Protzmann, A. R. Boyd, E. J. Thrush, J. Kappeler, M. Heuken, R. A. Talalaev, E. V. Yakovlev, A. V. Kondratyev, Modeling and process design of III-nitride MOVPE at near-atmospheric pressure in close coupled showerhead and planetary reactors, J. Crys. Growth, 298, 418-424 (2007)

[19] R. Singh, D. Doppalapudi, T.D. Moustakas, and L. T. Romano, Phase separation in InGaN thick films and formation of InGaN/GaN double heterostructures in the entire alloy composition, Appl. Phys. Lett. 70, 1089 (1997)

[20] Y. Nanishi, Y. Saito, T. Yamaguchi, M. Hori, F. Matsuda, T. Araki, A. Suzuki, and T. Miyajima, MBE-growth, characterization and properties of InN and InGaN, Phys. Stat. Sol. (a) 200, 202-208, (2003)

[21] M. Liao, Progress in Semicoductor diamond photodetectors and MEMS Sensors, Functional diamond 1, 29-46 (2021)

[22] L. Sang, M. Liao, M. Sumiya, X. Yang, Y. Koide, and B. Shen, In-rich InGaN solar cells with polarization induced hole doping in *p*-InGaN, submitted.

Figure caption

Figure 1 (a) XRD 2θ-ω scan in the (002) direction for the $In_{0.05}Ga_{0.95}N$ grown by high-pressure MOCVD, the inset is the cross-sectional SEM image; (b) AFM image of the $In_{0.05}Ga_{0.95}N$, showing good morphology; (c) XRD rocking curve around (002)-plane for $In_{0.05}Ga_{0.95}N$; (d) XRD rocking curve around (101)-plane for $In_{0.05}Ga_{0.95}N$.

Figure 2 Dependence of the (a) In mole fraction in the InGaN film and (b) growth rate grown at the pressure from 0.5 to 2.5 atms under the temperature of 830 °C. (c) and (d) are the mobilities and carrier concentrations of InGaN grown at different pressures.

Figure 3 The FWHM values of the XRD rocking curves for the (002) and (101)-plane as a function of the In mole fractions at different growth pressures.

Figure 4 (a1) The InGaN films grown at the pressure of 1 atm with different growth temperatures. (a2), (a3) and (a4) are the AFM images of the InGaN grown at 1 atm with the growth temperature of 720°C, 700°C, and 680°C, respectively. (b1) The InGaN films grown at the pressure of 2 atms with different growth temperatures. (b2), (b3) and (b4) are the AFM images of the InGaN grown at 2 atms with the growth temperature of 760°C, 780°C, and 824°C, respectively.

Figure 5 (a) The current density-voltage (*J-V*) and power density-voltage (*P-V*) characteristics of the solar cells under AM 1.5 solar simulator illumination; (b) EQE of solar cell dependent on the wavelength from 800 to 300 nm.

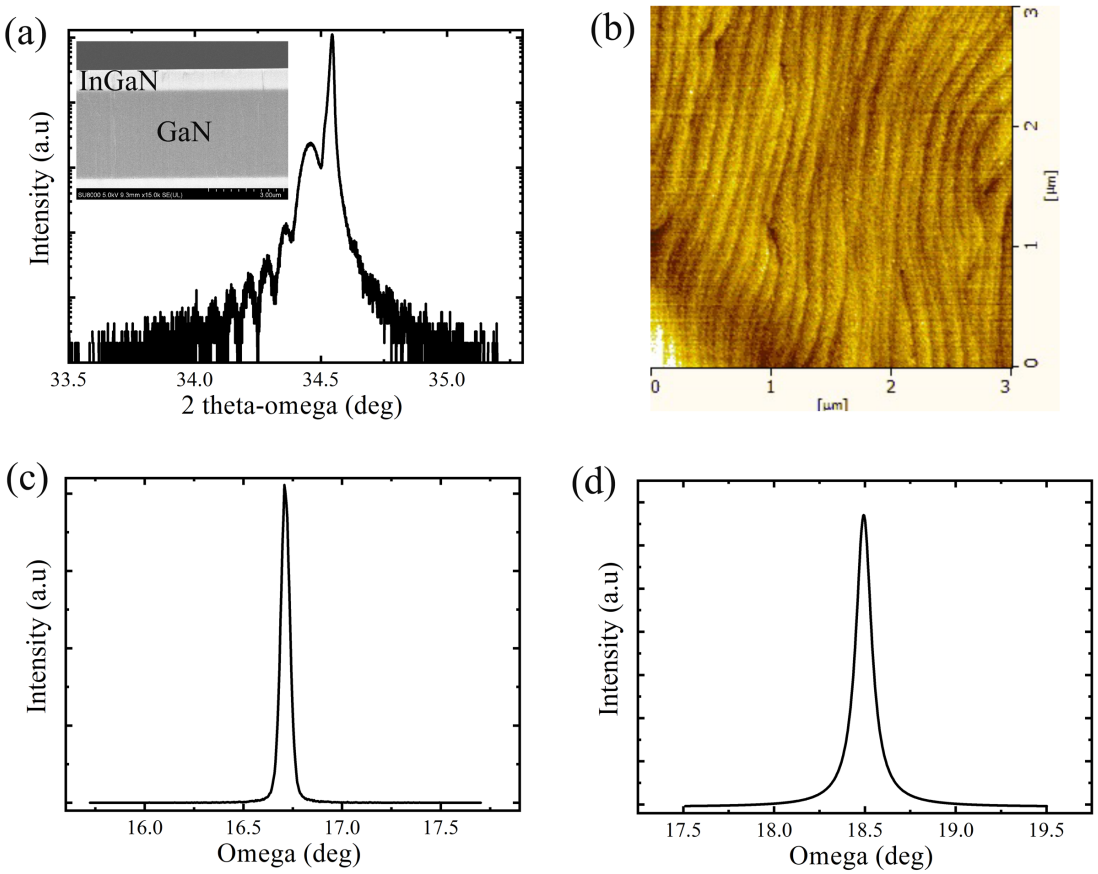
(a)
InGaN
GaN
Intensity (a.u)
33.5
34.0
34.5
35.0
2 theta-omega (deg)
(b)
0
1
2
3
[µm]
(c)
Intensity (a.u)
16.0
16.5
17.0
17.5
Omega (deg)
(d)
Intensity (a.u)
17.5
18.0
18.5
19.0
19.5
Omega (deg)

Fig. 1

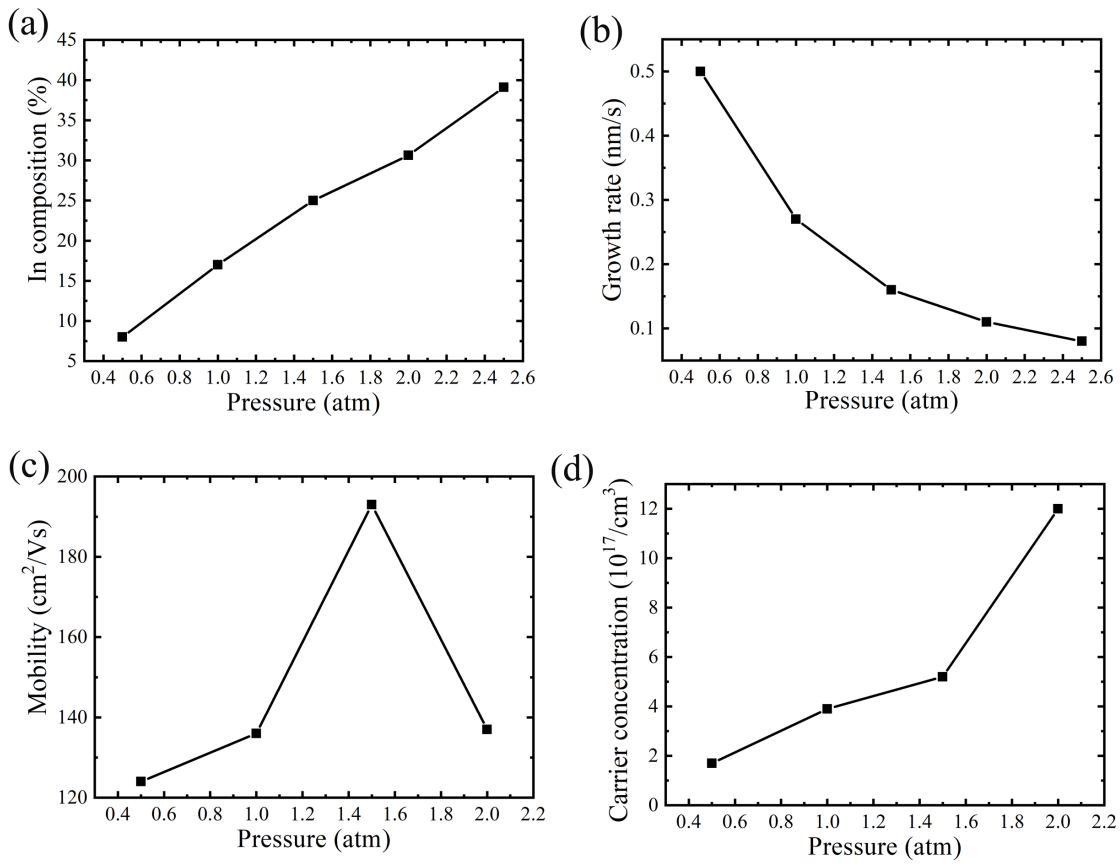
(a)
In composition (%)
Pressure (atm)
(b)
Growth rate (nm/s)
Pressure (atm)
(c)
Mobility (cm²/Vs)
Pressure (atm)
(d)
Carrier concentration (10¹⁷/cm³)
Pressure (atm)

Fig. 2

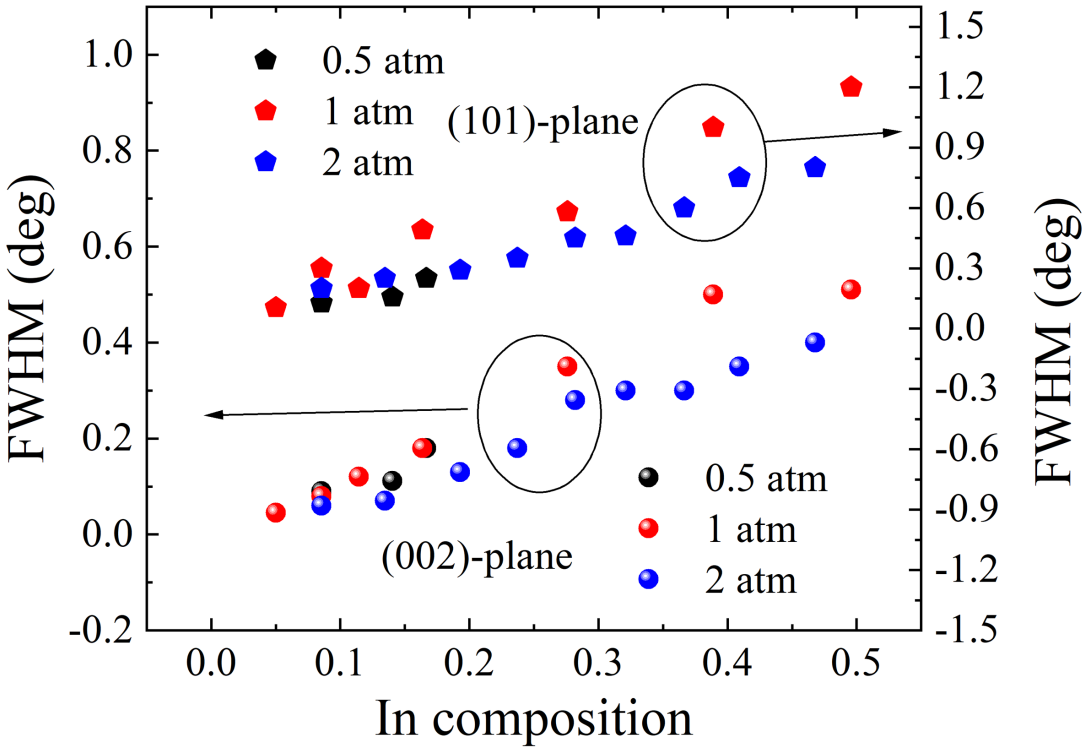
0.5 atm
1 atm
2 atm
(101)-plane
(002)-plane
0.5 atm
1 atm
2 atm
FWHM (deg)
FWHM (deg)
In composition
1.0
0.8
0.6
0.4
0.2
0.0
-0.2
1.5
1.2
0.9
0.6
0.3
0.0
-0.3
-0.6
-0.9
-1.2
-1.5
0.0
0.1
0.2
0.3
0.4
0.5

Fig. 3

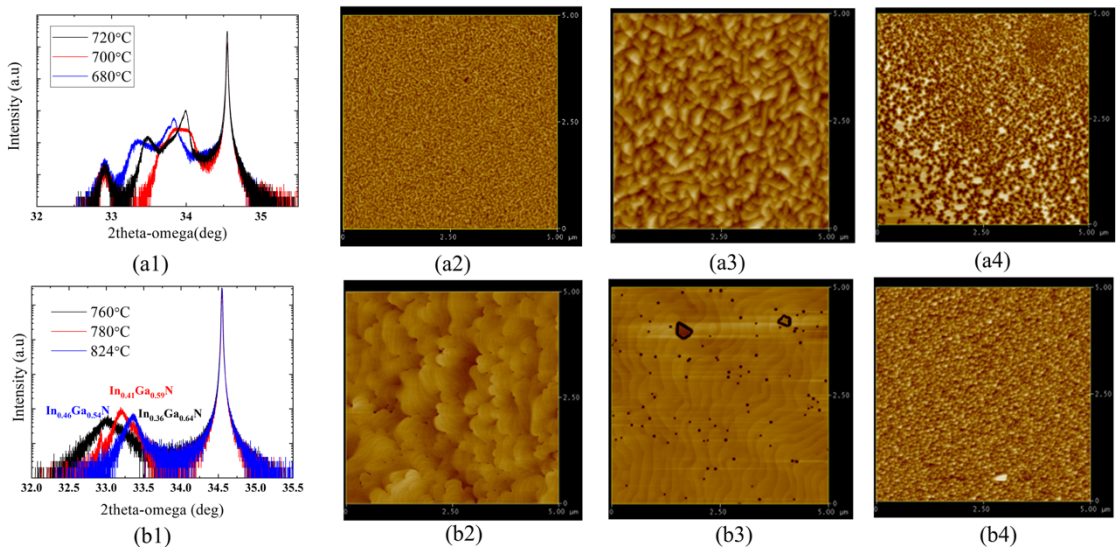
720°C
700°C
680°C
Intensity (a.u)
2theta-omega(deg)
(a1)
(a2)
(a3)
(a4)
760°C
780°C
824°C
Intensity (a.u)
$In_{0.41}Ga_{0.59}N$
$In_{0.46}Ga_{0.54}N$
$In_{0.36}Ga_{0.64}N$
2theta-omega (deg)
(b1)
(b2)
(b3)
(b4)

Fig. 4

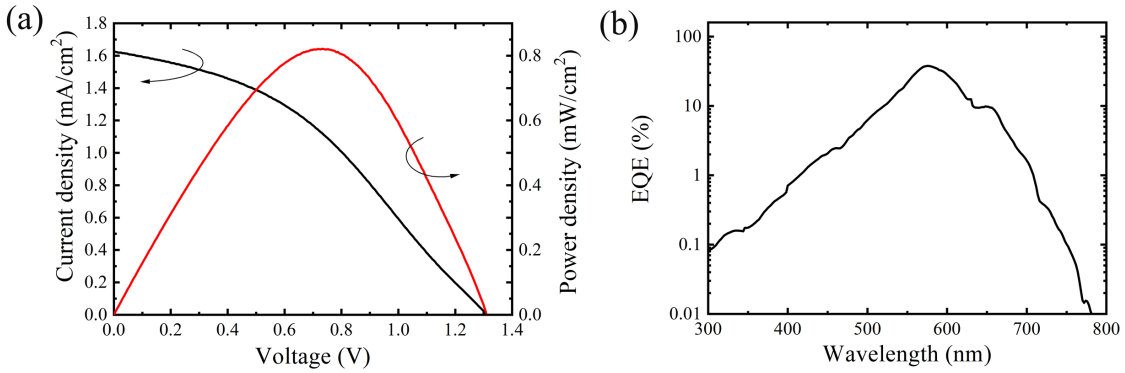
(a)
Current density (mA/cm^2)
Power density (mW/cm^2)
Voltage (V)
(b)
EQE (%)
Wavelength (nm)

Fig. 5